Liquid Optical Fibers with a Multistable Core Actuated by Light Radiation Pressure

Etienne Brasselet, Régis Wunenburger, and Jean-Pierre Delville
Centre de Physique Moléculaire Optique et Hertzienne, Université Bordeaux 1, CNRS, 351 Cours de la Libération, 33405 Talence Cedex, France
(Received 6 March 2008; published 30 June 2008)

We report on spatiotemporal behavior of self-adapted dielectric liquid columns generated and sustained by light radiation pressure. We show that single- or multivalued liquid column diameter depends on the excitation light beam. When the beam diameter is sufficiently small, we observe a well-defined stationary column diameter. In contrast, at a larger beam diameter, the liquid column experiences complex spatiotemporal dynamics whose statistical analysis evidences an underlying multistable structure. Experimental observations are all supported by a full electromagnetic model that accounts for the wave guiding properties of the liquid column viewed as a step-index liquid-core liquid-cladding optical fiber having an optically tunable core diameter.

DOI: 10.1103/PhysRevLett.101.014501 PACS numbers: 47.20.Ma, 42.25.Gy, 42.50.Wk, 82.70.Kj

By combining optics and microfluidics, optofluidics becomes an emergent research field offering an unprecedented level of integration to build a new generation of microdevices merging optical reconfigurability, smoothness of fluid interfaces, and the compactness of microchips [1]. If great achievements were realized in optical switching [2] and splitting [3], adaptive lensing [4,5], interferometry [6], and lasing [7], optical guiding by liquid fibers remains very challenging because stabilization of free-standing liquid columns encounters a fundamental limitation associated to the Rayleigh-Plateau instability [8]: In weightless conditions, a liquid column breaks when its length exceeds its circumference due to capillary forces. A method involving flow focusing in microchannels has thus been developed to build liquid-core liquid-cladding waveguides [9]. It offers a good level of control, since the refractive indices can be changed with the fluids and the size and the path of the liquid core can be varied with the fluid flow rates. Tunability cannot be nevertheless instantaneous, and optical guiding is not adapted to the incident light because both aspects are controlled externally by flow rates.

Strategies based on electric fields [10–12] and acoustic radiation pressure [13] have also been adopted to bypass the Rayleigh-Plateau instability of a static liquid column and have succeeded in slightly repelling the onset by less than a factor of 2. A few years ago, an optical technique relying on light radiation pressure [14] has demonstrated the unique ability to stabilize liquid columns with a very large aspect ratio and to offer self-adaptation to the laser wave used to form them, thus leading to tunability of the diameter column and adjustment of its direction. However, no theoretical explanation has been advanced so far to describe this behavior, and the mechanism ensuring the column stability and fixing the liquid optical fiber diameter still remained open issues.

In this work, we present dedicated experiments of radiation pressure sustained liquid columns with an aspect ratio up to 100 showing that either a single- or a multivalued column diameter may exist depending on the diameter and power of the light beam. Viewing a liquid column as a step-index optical fiber having an adaptable core diameter, we build an electromagnetic model that takes into account both its optical waveguiding properties and radiation pressure effects. The model predicts (i) the stability conditions of a liquid column sustained by light and (ii) that the monomodal or multimodal character of light propagation inside the liquid fiber is associated to the existence of monostable or multistable states. It is found to be in very good quantitative agreement with experimental observations, thus demonstrating a new mechanism of stabilization by light of two-phase liquid structures. The present results are the first demonstration of a self-adapted liquid-core liquid-cladding optical fiber. Moreover, its characteristics can be tuned by light at will.

Experiments are performed in a near-critical quaternary liquid mixture made of toluene, sodium dodecyl sulfate, *n*-butanol, and water with weight fraction 70%, 4%, 17%, and 9%, respectively. Details on the preparation of the solution can be found in Ref. [15]. For a temperature above the liquid-liquid critical temperature $T_C = 35\,^{\circ}\mathrm{C}$, this mixture separates into two transparent water-in-oil micellar phases labeled 1 and 2, whose interfacial surface tension σ vanishes as T_C is reached [15]. Since the density (index of refraction) of water is larger (smaller) than that of toluene, the micellar phase of larger concentration (phase 1) is located below the low micellar concentration (phase 2), while its refractive index n_1 is smaller than n_2. The experimental configuration is shown in Fig. 1(a). The mixture is enclosed in a $e = 1$ mm-thick fused quartz cell that is thermally controlled at $T = T_C + 2(\pm 0.05)$ K for which we have $n_1 = 1.444$, $n_2 = 1.460$, and $\sigma = 1.75 \times 10^{-7}$ N/m [16]. Close to T_C, phase 2, of height $e/2$, completely wets the cell walls [Fig. 1(a)].

A vertical downward linearly polarized Gaussian beam from a cw Ar^+ laser operating at wavelength $\lambda = 514.5$ nm is focused onto the interface by a microscope objective ensuring a cylindrical symmetry of the intensity

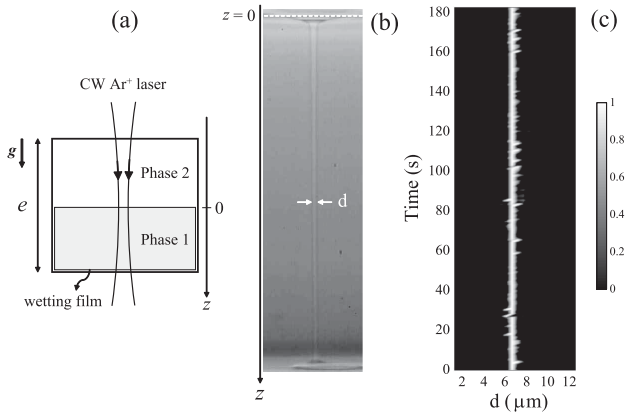

FIG. 1. (a) Experimental setup. The TEM_{00} mode of a cw argon ion laser operating at wavelength $\lambda = 514.5$ nm is focused at the fluid-fluid interface of the phase separated liquid mixture whose temperature is regulated above the critical temperature T_c. The less refractive phase, labeled 1, is the denser one. The cell thickness is $e = 1$ mm. (b) Typical liquid column with diameter d. (c) Dynamics of the diameter normalized probability along the column $\Lambda_z(d)/\max[\Lambda_z(d)]$, with $w_0 = 1.8$ μm and $P = 600$ mW.

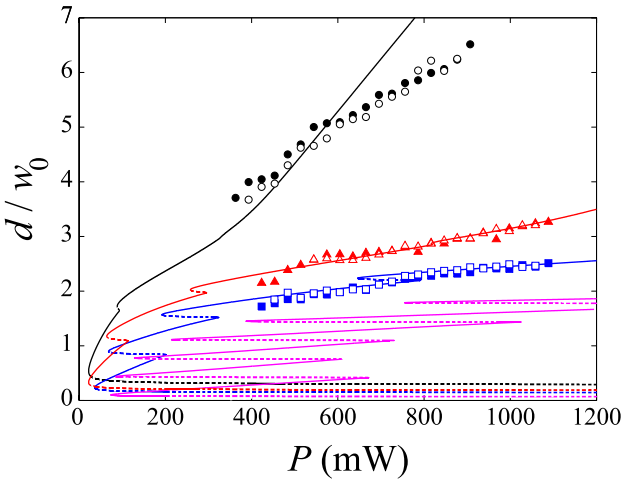

FIG. 2 (color online). Power dependence of the liquid fiber diameter for beam waists $w_0 = 1.8$ (black line and circles), 2.7 (red line and triangles), 3.5 (blue line and squares), and 7.0 μm (magenta). Solid and open symbols refer to increasing and decreasing power, respectively. Solid and dashed lines correspond, respectively, to stable and unstable states predicted by the model.

profile, as shown in Fig. 1(a). The intensity profile at $z = 0$ (i.e., the altitude of the unperturbed interface) is $I(r) = \frac{2P}{\pi w_0^2}\exp(-\frac{2r^2}{w_0^2})$, where P is the total beam power and w_0 is the beam waist. At a high enough power, typically hundreds of milliwatts, a perfectly beam-centered 0.5 mm-long liquid column of phase 2 forms between the interface and the wetting layer [Fig. 1(b)] following an optohydrodynamic instability [17].

For the smallest beam waists we used, $w_0 = 1.8$, 2.7, and 3.5 μm, a stable column with a well-defined diameter d is observed. The diameter probability distribution along the column $\Lambda_z(d)$ indeed exhibits a single-valued and stationary behavior, as shown in Fig. 1(c), where $w_0 = 1.8$ μm and $P = 600$ mW (the acquisition rate is 25 Hz in all experiments). The power dependence of the column diameter for such structures having a stable and well-defined diameter is summarized in Fig. 2, where the solid and open symbols refer to increasing and decreasing power, respectively. We conclude that no memory effect is observable. This means that d is unambiguously defined once w_0 and P are fixed within the explored range of parameters. However, we observe a strong nonlocal effect since, at fixed power, the ratio d/w_0 increases when the spatial extension of the excitation beam w_0 is decreased. Such a dependence is nontrivial and requires us to look at the light-matter interaction in some details. Our approach consists of considering the column as a liquid step-index optical fiber with self-adaptable core, where phase 1 and 2 play the role of the clad and the core, respectively, recalling that $n_1 < n_2$. On the one hand, it is clear that such a liquid fiber does not collapse due to the radially inward acting Laplace pressure because of the radially outward competing light radiation pressure. On the other hand, it is known that the power injection and the resulting modal structure of the optical field inside a fiber strongly depends on its characteristics, namely, the refractive index contrast between the clad and the core, the core diameter, and the beam waist at the entrance of the fiber [18]. Therefore, in order to quantitatively describe the self-adapted liquid optical fiber sustained by light radiation pressure, one has to simultaneously solve the following coupled problems that are (i) the injection of the Gaussian incident beam into the fiber, (ii) the light propagation inside the fiber, and (iii) the balance of the involved forces. An overview of our model and its main results are given below. More details will be found in a forthcoming publication.

We consider the liquid column as a semi-infinite cylinder of radius $R = d/2$ perfectly aligned with the incident excitation beam, the inner and outer refractive indices being n_2 and n_1, respectively. Since $n_1 \simeq n_2$, the modes that propagate inside the column can be described satisfactorily by the linearly polarized LP_{lm} modes [18], and only the first-order terms in $n_2 - n_1$ can be retained in the calculations. Since the incident beam is Gaussian, the coupling to modes with $l \geq 1$ is zero and only the LP_{0m} modes are excited, each of them carrying a power $P_m = T_m P$, where T_m is the coupling coefficient. The transmission for the mth mode is calculated from the normalized overlap integral between the incident Gaussian field and the propagating LP_{0m} field:

$$T_m = \frac{8}{w_0^2 R^2}\frac{|\int_0^\infty \mathcal{R}_m(r)e^{-(r^2/w_0^2)}rdr|^2}{\frac{J_1^2(\kappa_m R)}{J_0^2(\kappa_m R)} + \frac{K_1^2(\gamma_m R)}{K_0^2(\gamma_m R)}}, \quad (1)$$

where J_n and K_n are the usual Bessel functions and κ_m and γ_m are the mth roots of the characteristic equation that defines the LP_{0m} mode, $\kappa_m \frac{J_1(\kappa_m R)}{J_0(\kappa_m R)} = \gamma_m \frac{K_1(\gamma_m R)}{K_0(\gamma_m R)}$, where $(\kappa_m)^2 + (\gamma_m)^2 = (2\pi/\lambda)^2(n_2^2 - n_1^2)$ [18]. The function $\mathcal{R}_m(r)$ is associated to the radial profile of the electric field of the mode m:

$$\mathcal{R}_m(r) = \left(\frac{J_0(\kappa_m r)}{J_0(\kappa_m R)} \Big|_{r \le R}, \frac{K_0(\gamma_m r)}{K_0(\gamma_m R)} \Big|_{r \ge R} \right). \quad (2)$$

In weightless conditions for steady and perfectly cylindrical columns, the interface equilibrium condition writes $\Pi_{\text{radiation}} = \Pi_{\text{Laplace}}$, where $\Pi_{\text{Laplace}} = \sigma/R$, since the viscous stress due to a possible flow within a perfect cylinder is tangential to the interface. The radiation pressure $\Pi_{\text{radiation}}$ corresponds to the radial discontinuity of the electromagnetic stress tensor [19] across the normal to the interface. In the present situation involving nonmagnetic fluids, to the lowest order in $n_2 - n_1$, we get

$$\Pi_{\text{radiation}} = \frac{1}{2} \epsilon_0 \bar{n} (n_2 - n_1) \sum_m |\mathbf{E}^{(m)}|^2_{r=R}, \quad (3)$$

where $\bar{n} = (n_2 + n_1)/2$ is the averaged refractive index, ϵ_0 the vacuum permittivity, and $\mathbf{E}^{(m)}$ the complex electric field of the mode m. Then, since the flux of the z component of the Poynting vector across a plane perpendicular to the z axis equals the power carried by the mth mode $P_m = T_m P$, we deduce that

$$|\mathbf{E}^{(m)}|^2_{r=R} = \frac{2P_m}{\epsilon_0 \pi c \bar{n} R^2} \left[\frac{J_1^2(\kappa_m R)}{J_0^2(\kappa_m R)} + \frac{K_1^2(\gamma_m R)}{K_0^2(\gamma_m R)} \right]^{-1}. \quad (4)$$

Finally $\Pi_{\text{radiation}}$ is explicitly obtained by combining Eqs. (1), (3), and (4).

The column diameter is further found by numerically solving the equilibrium equation. The model predicts that there is no equilibrium radius below a critical power and a discrete set of solutions $\{R_{\text{eq}}^{(n)}\}$ above. The stability criterion is obtained from a standard statics stability analysis at $R = R_{\text{eq}}^{(n)}$ and leads to $\partial \Pi_{\text{radiation}}/\partial R < \partial \Pi_{\text{Laplace}}/\partial R$. Results are displayed in Fig. 2, where the solid (dashed) line refers to stable (unstable) solutions. As far as the smallest waists are considered (i.e., like those presented in Fig. 2), a good quantitative agreement with experimental data is obtained, especially since no adjustable parameter is used. A more complex sequence of stable and unstable states is predicted at lower power, but this region cannot be explored experimentally since the large aspect ratio column detaches from the wetting film at the bottom of the cell. Note finally that a single and well-defined diameter does not imply a monomodal (i.e., $m = 1$ only) behavior. Indeed, as an example, the numbers of modes involved in the range of parameters presented in Fig. 2 are $m_{\max} = 6$ and 4 for $w_0 = 1.8$ and 2.7 μm, respectively.

When the beam waist is sufficiently large, the model predicts multistable states as shown in Fig. 2, where the results for $w_0 = 7$ μm are shown in magenta. There are indeed several stable radii at fixed power that should correspond to several observable column diameters. One would expect to experimentally observe metastable states as well as a hysteretic behavior of $d(P)$. We rather observe a column whose diameter varies along z and with time t, in distinction to what is found for smaller waist [Figs. 1(b) and 1(c)]. This point is detailed in Fig. 3 for $w_0 = 7$ μm and $P = 575$ mW at a fixed time. The column diameter as a function of z is shown in Fig. 3(a), the corresponding picture being shown in Fig. 3(b). The instantaneous diameter probability distribution $\Lambda_z(d)$ along the column is shown in Fig. 3(c). The distribution $\Lambda_z(d)$ is obtained by using the fit of $d(z)$ shown in Fig. 3(a), which appears as a red solid line. Typically, $\Lambda_z(d)$ exhibits two distinct peaks, labeled d_1 and d_2 in Fig. 3(c). Note that $d_{1,2} \sim (1.5\text{–}2)w_0$ and their difference $(d_2 - d_1) \sim 0.4 w_0$ compare well to the predicted values shown in Fig. 2. The system explores different discrete diameter values at a single time, which is the signature of the bistability (or multistability) predicted by our steady-state model. The mean amplitude of thermal fluctuations of the local interface position $(k_B T/\sigma)^{1/2} \sim 0.1\text{–}0.2$ μm [20], where $k_B T$ is the thermal energy, is 1 order of magnitude smaller that the interplateaux distance, thus eliminating departure from a perfect cylinder by pure thermal activation. However, the coupling between these thermal fluctuations and the weak light-induced flow inside the liquid column [21] can give birth to a viscous stress normal to the interface and the subsequent exploration of multivalued fiber radii for large beam diameters. This signature is further strengthened by the overall increase of the set of discrete diameter values with power, which we study below by taking advantage of the long-term stationarity of the system to improve the signal-to-noise ratio of the diameter statistical distribution.

To this purpose, we introduce the most probable diameter d^* as the diameter corresponding to the maximum of $\Lambda_z(d)$ at a fixed time t. For example, we have $d^* = d_2$ for the picture analyzed in Fig. 3(c). By doing so, from a movie

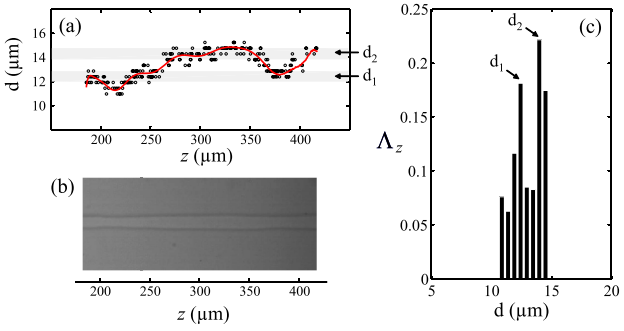

FIG. 3 (color online). (a) Column diameter along the z axis. Symbols refer to image analysis contour detection, and the red line is a suitable smooth fit of experimental data. (b) Picture that corresponds to (a). (c) Diameter probability distribution along the column, at a fixed time, using the fitted diameter data shown in (a). The beam waist is $w_0 = 7.0$ μm and $P = 575$ mW.

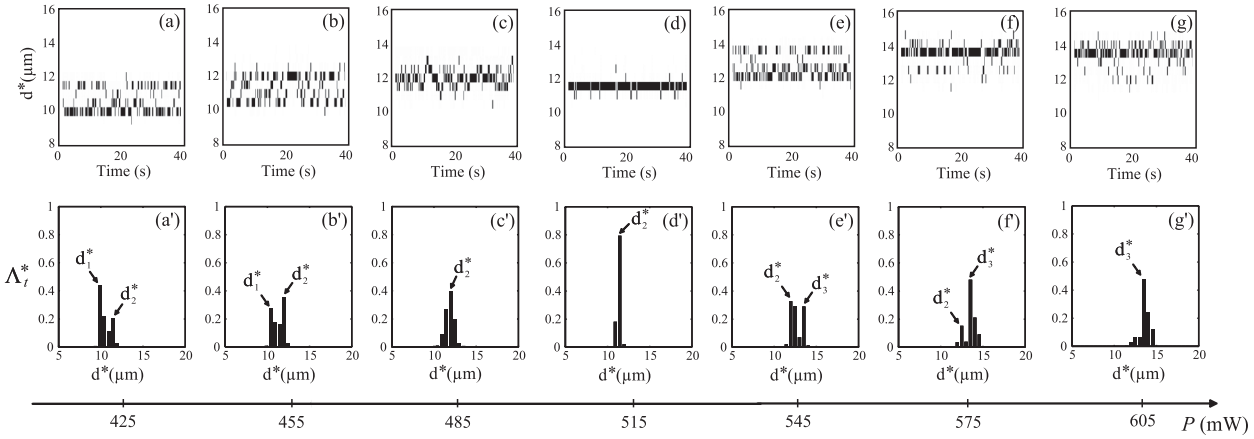

FIG. 4. Upper panels: Dynamics of the most probable diameter d^* with $w_0 = 7.0$ μm. Bottom panels: Probability distribution of d^* over a time window of 200 s. Panels (a, a′)–(g, g′) correspond to powers $P = 425$, 455, 485, 515, 545, 575, and 615 mW, respectively.

of the time-dependent column recorded at fixed power, we construct a time-dependent signal of the most probable column diameter $d^*(t)$. The power dependence of $d^*(t)$ is shown in Figs. 4(a)–4(g). As noted above, we observe that the trend of $d^*(t)$ is to increase with P in agreement with the statics model tendency.

Interestingly, depending on the power, $d^*(t)$ either is almost time-independent [Figs. 4(d) and 4(g)] or exhibits a double-valued behavior [Figs. 4(a)–4(c), 4(e), and 4(f)]. This is supported by the aspect and the power dependence of the probability distribution of $d^*(t)$, $\Lambda_t^*(d^*)$, shown in Figs. (4a′)–(4g′). As P is increased from 425 [Fig. 4(a)] to 515 mW [Fig. 4(d)], the height of the probability peak corresponding to d_1^* progressively decreases while the one corresponding to d_2^* increases. The same behavior is observed between 515 and 605 mW, showing the reproducibility of this trend. So, in experimental conditions for which the steady-state equilibrium model predicts a multistable behavior of d versus P resulting from successive subcritical bifurcations, the observed most probable column diameter d^* is time-dependent and takes only discrete values. Only the probability of observation of these discrete d^* values continuously depends on P. This statistical analysis allowed by the time dependence of the columns diameter thus evidences the underlying multistable behavior predicted by the steady-state equilibrium model. It also explains why no diameter hysteresis could be observed. In fact, the observed interface fluctuations make the column investigate its allowed steady states, thus preventing the column from staying in a metastable state, in a very similar way to noise-induced bistability in the presence of a subcritical bifurcation [22].

In conclusion, we have demonstrated the mechanism by which liquid columns of large aspect ratio can be sustained by light. We showed that column stability occurs above a beam power threshold and described the self-adaptation to the incident exciting light wave. At a large beam waist, this adaptation becomes multivalued in agreement with experiments. The column stabilization well above the onset of the Rayleigh-Plateau instability and the self-adaptation of the liquid fiber core diameter to the incident beam whatever its power and waist open a promising route toward reconfigurable light guiding applications of great versatility.

[1] D. Psaltis, S. R. Quake, and C. Yang, Nature (London) **442**, 381 (2006).
[2] K. Campbell *et al.*, Appl. Phys. Lett. **85**, 6119 (2004).
[3] N. T. Nguyen *et al.*, J. Micromech. Microeng. **17**, 2169 (2007).
[4] A. Casner and J. P. Delville, Opt. Lett. **26**, 1418 (2001).
[5] D. Y. Zhang, N. Justis, and Y. H. Lo, Appl. Phys. Lett. **84**, 4194 (2004).
[6] C. Grillet *et al.*, Opt. Express **12**, 5440 (2004).
[7] Z. Li *et al.*, Opt. Express **14**, 696 (2006).
[8] J. Eggers, Rev. Mod. Phys. **69**, 865 (1997).
[9] D. B. Wolfe *et al.*, Proc. Natl. Acad. Sci. U.S.A. **101**, 12 434 (2004).
[10] H. Gonzalez *et al.*, J. Fluid Mech. **206**, 545 (1989).
[11] C. L. Burcham and D. A. Saville, J. Fluid Mech. **405**, 37 (2000).
[12] M. J. Marr-Lyon *et al.*, Phys. Fluids **12**, 986 (2000).
[13] M. J. Marr-Lyon, D. B. Thiessen, and P. L. Marston, Phys. Rev. Lett. **86**, 2293 (2001).
[14] A. Casner and J. P. Delville, Europhys. Lett. **65**, 337 (2004).
[15] A. Casner and J. P. Delville, Phys. Rev. Lett. **87**, 054503 (2001).
[16] H. Chraïbi *et al.*, Eur. J. Mech. B, Fluids **27**, 419 (2008).
[17] A. Casner and J. P. Delville, Phys. Rev. Lett. **90**, 144503 (2003).
[18] K. Okamoto, *Fundamentals of Optical Waveguides* (Elsevier, Amsterdam, 2006), 2nd ed.
[19] L. Landau and E. Lifschitz, *Electrodynamics of Continuous Media* (Pergamon, Oxford, 1984).
[20] D. G. A. L. Aarts, M. Schmidt, and H. N. W. Lekkerkerker, Science **304**, 847 (2004).
[21] R. D. Schroll *et al.*, Phys. Rev. Lett. **98**, 133601 (2007).
[22] S. Residori *et al.*, Phys. Rev. Lett. **88**, 024502 (2001).